Experimental study on performance of sand filter layer to remove non-point source pollutants in rainwater

Jaeyoon Ahn, Dongseop Lee, Shinin Han, Youngwook Jung, Sangwoo Park and Hangseok Choi

ABSTRACT

Clogging characteristics of conventional sand filter layers with different grain-size distributions were experimentally studied to estimate their filtration capacity to capture non-point source pollutants in an artificial rainwater reservoir. A series of laboratory-scale chamber tests was conducted for artificial urban runoff synthesized with non-point source pollutants collected from a real road in Seoul, Korea. In addition, an analytical filtration model for estimating removal of non-point source pollutants was adopted considering the clogging characteristics. To evaluate the performance of three types of sand filter layers with different grain size characteristics, the pollutant concentration was measured in terms of total suspended solids and chemical oxygen demand. The lumped parameter (θ) related to the clogging property was estimated by comparing the accumulated weight of pollutant particles obtained from the laboratory chamber experiments and the theoretical estimation from the analytical filtration model. Based on the experimental study and theoretical consideration, a double-sand-filter layer consisting of two separate layers is proposed as the optimum system for removing non-point source pollutants in the pilot-scale rainwater reservoir.

Key words | clogging, lumped parameter, non-point source pollutant, rainwater utilization, sand filter

Jaeyoon Ahn
Shinin Han
Youngwook Jung
R&D Center,
Seoyoung Engineering Corp.,
Seongnam-si,
Gyeonggi-do,
Korea

Dongseop Lee
Hangseok Choi (corresponding author)
School of Civil, Environmental, and Architectural Engineering,
Korea University,
Seoul,
Korea
E-mail: *hchoi2@korea.ac.kr*

Sangwoo Park
Department of Civil and Environmental, Engineering,
Sejong University,
Seoul,
Korea

INTRODUCTION

There have been a great many attempts to study rainwater harvesting and runoff reduction facilities, focusing on natural hydraulic cycles, in order to manage environmental problems due to the abnormal climate in densely populated urban areas. The Korean government applies the concept of low impact development (LID) for rainwater storage and infiltration, which is an eco-friendly urban development concept of maintaining water circulation as naturally as possible even after the development. As one of the LID strategies, a distributed rainwater reservoir can be installed in the subsurface of the urban sidewalk and parking lot pavements to reduce storm water runoff (Schuetze 2013; Liu *et al.* 2015). This artificial underground reservoir is required to be equipped with a filtering system to remove non-point source pollutants that are commonly contained in the first flush of rainfall in the urban areas, because a large amount of non-point source pollutants exists in the initial rainwater runoff from urban areas (John & Steven 1997; Barrett *et al.* 1998; Torben *et al.* 1998; Baek *et al.* 2015).

In this paper, among various proposed methods to remove non-point source pollutants, a sand filtration technique is selected to develop the optimized removal process, which can be assembled in the distributed rainwater reservoir. The excellence of the removal efficiency and economic applicability of the sand filtration technology were reported in several preceding studies (Seigrist & Boyle 1987; Bahgat *et al.* 1999; Rodgers *et al.* 2004; Cho *et al.* 2009; Nair *et al.* 2014; Lee *et al.* 2016). The pore-size distribution of the sand filter medium should be matched with the size distribution of pollution particles to enhance the

doi: 10.2166/ws.2017.056

removal efficiency of the non-point source pollutants (Stark *et al.* 2004; Hsieh & Davis 2005; Nguyen *et al.* 2011; Anggraini *et al.* 2014; Kandra *et al.* 2014).

During the operation period of a distributed rainwater reservoir, repeated occurrences of storm runoff may cause fine pollution particles to be gradually accumulated within the pores of the sand filter layer due to the effect of filtration and adsorption. As the accumulation process continues in the course of purification performance, the porosity and permeability of the sand filter layer gradually reduces and eventually leads to a significant decrease in the discharge of storm runoff (Kim *et al.* 2009).

An analytical filtration model for estimating removal of non-point source pollutants was adopted in this paper with consideration of the clogging characteristics of the sand filter layer such as the grain-size distribution and composition, and the variation in hydraulic conductivity and porosity. In order to verify the analytical filtration model, a series of laboratory-scale chamber tests was performed for three different sand filter layers with different grain size characteristics and compositions. The sand filter was permeated with artificial urban runoff synthesized with non-point source pollutants that were collected from a real road in Seoul, Korea. The performance of the sand filter layers was evaluated in terms of total suspended solids (TSS) and chemical oxygen demand (COD) as the index of non-point source pollutants. The effect of the lumped parameter (θ) on the clogging phenomenon of pollutant particles was estimated by comparing the accumulated weight of non-point source pollutants obtained from the laboratory chamber experiments and the theoretical estimation from the analytical model.

Based on the experimental study and theoretical consideration of clogging characteristics, the optimum configuration of the sand filter layer was proposed to construct a pilot-scale rainwater reservoir in a test bed. In addition, the removal efficiency of non-point source pollutants contained in the first flush with a rainfall intensity of 5 mm was evaluated to verify its field applicability. Most previous studies concentrate on the performance of laboratory experiments on a small scale, and there are few experimental studies regarding the natural characteristics of the filter media itself. However, the aim of this paper is to present an experimental program to identify the performance of sand filters, including not only conducting laboratory experiments but also verifying the model through the field-sized tests. In addition, a prediction model for removing the non-point source pollutants was proposed in order to design the sand filters in LID structures for utilizing rainwater.

ANALYTICAL FILTRATION MODEL FOR POLLUTANT REMOVAL IN SOIL FILTER LAYER

Reddi & Bonala (1997) investigated the filtration phenomenon where pores in the sand filter layer are clogged with suspension passing through the filter. Lee *et al.* (2004) proposed a systematic procedure to calculate the amount of clogged particles from the filtration model. It is assumed that filtration occurs by steady state flow of suspension with a constant initial concentration on the outside boundary of the porous media. The governing equation to represent particle migration per unit volume was expressed by Gruesbeck & Collins (1982) as follows:

$$\frac{\partial C}{\partial t}(\eta C + \eta_i \sigma) + V\frac{\partial C}{\partial Z} = 0 \tag{1}$$

where C is the particle concentration in suspension, η_i is the initial porosity, η is the porosity after particle deposition, σ is the mass of deposited particles per unit pore volume, v is the discharge velocity, z is the one-dimensional coordinate, and t is the time.

Equation (1) can be simplified as follows (Lee *et al.* 2004):

$$\frac{\partial C}{\partial t} + V\frac{\partial C}{\partial z} + \frac{\partial \sigma}{\partial t} = 0 \tag{2}$$

where V is the seepage velocity (v/η). The third term on the left-hand side of Equation (2) can be expressed as Equation (3) with consideration of particle adsorption according to particle concentration in the suspension (Ives 1987). Therefore, Equation (2) can be replaced by Equation (4).

$$\frac{\partial \sigma}{\partial t} = \lambda C \tag{3}$$

$$\frac{\partial C}{\partial t} + V\frac{\partial C}{\partial z} + \lambda C = 0 \tag{4}$$

where λ is the particle deposition coefficient.

The deposition of fine particles per unit pore volume in the filter layers (that is $\sigma(z, t)$), which is expressed as a function of time and space, can be obtained from Equation (4). The total weight of fine particles ($W(z, t)$) deposited in the filter layers is calculated as follows:

$$W(z,t) = \int_0^z \lambda C_i e^{-(\lambda z/V)}\left(t - \frac{z}{V}\right)\cdot A_v dz \tag{5}$$

where A_v is the pore area ($A_v = A \cdot n$). Lee *et al.* (2004) expressed $W(z, t)$ in terms of time and space variables as follows:

$$W(z,t) = \left[\frac{z}{V}\cdot\exp\left(\frac{-\lambda z}{V}\right) + \frac{1}{\lambda}\cdot\exp\left(\frac{-\lambda z}{V}\right) - t\cdot\exp\left(\frac{-\lambda z}{V}\right) + t - \frac{1}{\lambda}\right]\cdot V\cdot C_i\cdot A\cdot n \tag{6}$$

In order to obtain $W(z, t)$ from Equation (6), the particle deposition coefficient (λ) should be evaluated in advance and shows the relationship between the concentration of suspension and the deposition amount (Kim *et al.* 2009). Reddi & Bonala (1997) suggested a theoretical way to obtain the particle deposition coefficient by means of the particle capture probability approach as follows:

$$\lambda = \frac{V}{\alpha^* e^{2(b^2+m)}}\left[4K_1 - 4K_2 e^{((b^2-2m)/2)} + K_3 e^{2(b^2-m)}\right] \tag{7}$$

where α^* indicates the effective length of cylindrical pore tubes, m is the mean value of the log normal distribution of pore radius, b is the standard deviation of the log normal distribution of pore radius, K_1, K_2 and K_3 are expressed by the lumped parameter (θ) and the particle size (α) in suspension as $K_i = (\theta\alpha)^{i+1}$ where $i = 1$, 2 and 3.

A constant value of λ/V can be obtained from Equation (7), which is a key factor governing the distribution of particle deposition (Kim *et al.* 2009; Nieć *et al.* 2016). Putting λ/V into Equation (6), the total weight of fine particles deposited in the filter layers with time can be calculated. The lumped parameter (θ) overall relates to the gravitational, inertial, hydrodynamic, electric and van der Waals forces acting on the particles in suspension (Gruesbeck & Collins 1982; Rege 1988; Rege & Fogler 1988). Figure 1 depicts the probability of particle capture in a pore tube, in which the larger the value of θ, the broader the dotted line range, showing that the suspended particles can deposit easily in the pore tubes, and the particle deposition increases. Rege & Fogler (1988) suggested the range of θ from 1 to 10 based on the laboratory experiments for bentonite suspension with a varied concentration of KCl (i.e., 0 to 0.01).

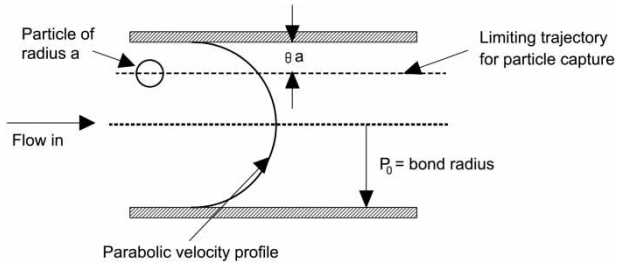

Figure 1 | Probability of particle capture in pore tube equivalent to the fraction of total flow in annulus between r and (r-θ a) (from Rege & Fogler 1988).

In this paper, the lumped parameter (θ) to obtain λ/V was determined by analyzing the laboratory chamber tests for the sand filter layers. That is, θ was estimated by comparing the value of $W(z, t)$ calculated from Equation (6) and the accumulative weight of clogged pollutant particles in the sand filter layers measured from the laboratory-scale chamber tests.

TEST MATERIALS

Characteristics of non-point source pollutants

To assess the removal efficiency of the sand filter layers for non-point source pollutants, the sand filter was permeated with artificial urban runoff synthesized with non-point source pollutants that were collected from a real road in Seoul, Korea. Dry non-point source pollutants sampled from real automobiles were sieved with a 10-mm-diameter sieve to remove trash and fallen leaves. After the first sieving, the dry non-point source pollutants were sieved again with a 0.25-mm-diameter sieve (i.e., No. 60 sieve) to prepare the dry pollutant sample that was mixed with water

corresponding to about 4% of the total non-point source pollutants by weight. Figure 2 shows the condition of non-point source pollutants and the preparation procedure for the dry sample. Using the prepared non-point source pollutants sample, the sieve analysis and the fundamental physical property tests were conducted. Figure 3 shows the first and second sieved grain size distribution curves for the non-point source pollutants samples. Table 1 summarizes the fundamental properties of the non-point source pollutants sample.

A series of component analysis tests was performed to quantitatively identify the contaminant components and their contents (i.e., polycyclic aromatic hydrocarbons (PAHs), phenol, nitrogen, phosphorus, and heavy metals) in the non-point source pollutants, which was adopted in previous studies (Wilson *et al.* 2014; Kim *et al.* 2016). Table 2 shows the quantity of components detected in the dry sample along with the analysis method and the test equipment. In addition, the quantity of inorganic contaminants was evaluated in terms of TSS and COD in the course of the laboratory-scale chamber tests.

PAHs are typically detected from rainfall runoff in the city area. Skin contact with PAHs causes toxic responses, and ingestion can cause cancers at extremely low concentrations. For example, PAHs have the dangerous potential of 10^{-6} for cancer to occur with the PAHs concentration of 9.7×10^{-4} mg/L (Choi & Shin 1997). The standard criterion for PAHs of the US Environmental Protection Agency (EPA) for drinking water from surface water resources is a concentration of 0.028 mg/L (US EPA 1983). In the component analysis test of the non-point source pollutants, prevalent PAHs such as benzo(a) pyrene (2.565 mg/kg), fluoranthren (0.855 mg/kg) and pyrene (0.75 mg/kg) were detected to be about 260–900 times higher than the EPA criterion.

Toxic phenolic compounds are commonly discharged from heavy industries such as coal energy, metal casting, and paper production and classified as a hazardous pollution group (Caza *et al.* 1999). Diverse preceding studies show the heredity and immunity toxic effects, and the carcinogenicity of phenol has been reported. It is obvious that phenol has a fatal influence on the natural environment and human health (Hori *et al.* 2006). The water quality standard for drinking water from the Ministry of Environment, Korea, sets a limit for phenol concentration of 0.005 mg/L. However,

Figure 2 | Preparation of dry sample of non-point source pollutants: (a) collection of non-point source pollutants, (b) first sieve separation, and (c) dry sample of non-point source pollutants after second sieve separation.

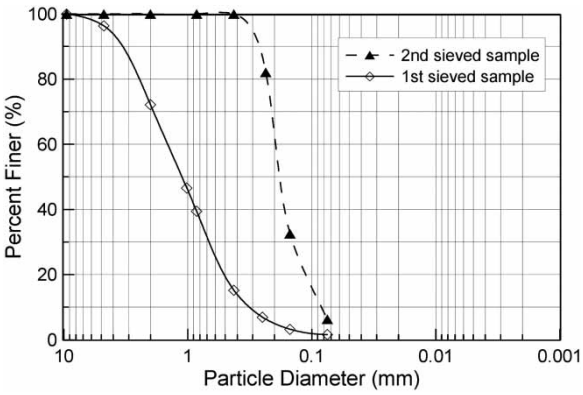

Figure 3 | Grain size distribution curves for non-point source pollutants samples.

Table 1 | Material properties of non-point source pollutants sample

Effective size (D_{10}, mm)	Specific gravity (G_s)	Liquid limit (*LL*, %)	Plastic limit (*PL*, %)	Plastic index (*PI*, %)	Soil classification
0.085	2.49	NP			SP

NP, Non-plastic; SP, Poorly-graded sand.

phenol and pentachlorophenol in the non-point source pollutants were measured at 4 mg/kg and 1.79 mg/kg, respectively, which are about 800 times higher than the standard.

Nitrogen and phosphorus exist as organic compounds in the natural condition. They cause serious eutrophication, discoloration of water, and effluvium from decomposition. T-P, which is the phosphorus component, was measured to be 199.125 mg/kg and in the nitrogen components, T-N (1,967 mg/kg), NH_4-N (84 mg/kg), NO_3-N (11.2 mg/kg), and TKN (1,955.8 mg/kg) showed significantly high levels together with T-P.

The representative heavy metal components also exist such as aluminum, arsenic, copper, cadmium, mercury, nickel, zinc, chrome and lead. In particular, mercury, copper, and lead are known to cause fatal problems in human health. In the component analysis tests for heavy metals, aluminum (5,826 mg/kg) and zinc (834 mg/kg) showed very high levels and mercury (0.505 mg/kg), lead (77.644 mg/kg), and copper (121.902 mg/kg) also revealed relatively high values. Table 3 summarizes the average concentration of heavy metals detected from rainfall runoff according to land use in the city areas of the USA (Pitt & Barron 1990). Pitt and Barron's research suggests that a large quantity of heavy metals was mainly detected in the city areas such as industrial sites, roads, and parking lots. It was verified that the amount of heavy metals included in

Table 2 | Component analysis result of non-point source pollutants sample

Component		Value (mg/kg)	Analysis method	Measuring equipment
PAHs	Benzo(a) pyrene	2.565	EPA Method 8270 C	GC-MSD (Gas Chromatography–Mass Selective Detector) 7890A/ 5975C (Agilent)
	Fluoranthren	0.855		
	Pyrene	0.750		
Phenols	Phenol	4	EPA Method 8041	GC-FID (Gas Chromatography–Flame Ionization Detector) 7890A (Agilent)
	Pentachlorophenol	1.790		
P	T-P	199.125	EPA Method 365.1/Ascorbic Acid	UV-Vis (Ultraviolet-Visible) Lambda25 (Perkin Elmer)
N	T-N	1,967	Standard Method 4500-Norg	
	NO_3-N	11.2		
	TKN	1,955.8		
	NH_4-N	84	Standard Method 4500-Norg/ Titration	–
Heavy metals	Al	5,825.5	EPA Method 6010 B	ICP-OES (Inductively Coupled Plasma–Optical Emission Spectra) Optima 7300 DV (Perkin Elmer)
	As	2.496		
	Cu	121.902		
	Cd	1.364		
	Hg	0.505		
	Ni	19.319		
	Zn	833.795		
	Cr	55.028		
	Pb	77.644		
	Hg	0.505	EPA Method 7473	Direct Mercury Analyzer DMA-80 (Milestone)

Table 3 | Average concentration of metals in storm water in urban areas of USA (Pitt & Barron 1990)

Pollutants (mg/L)	Residence/Industry Street	Industry area Street	Residential area Parking lot	Commerce/Industry Parking lot	Industry/Unpave A, Parking lot	Industry/Unpave B, Parking lot
Al	181	4,520	2,500	558	11,600	3,140
Cd	0.46	55.7	35.3	2.6	–	1
Cr	3	11	290	19.6	1.5	6.5
Cu	10	410	285	39.3	390	13.3
Pb	15.8	56.3	66.7	45.4	65.5	28
Ni	2.23	19.9	35.3	33.1	30	73.3
Zn	37.5	67.5	64	178	81.5	28.3

the dry sample of non-point source pollutants in this study is similar to the results of Pitt & Barron (1990).

Characteristics of sand filter layers

In this paper, two sand samples were selected as a filtering component of the sand filter layers. The sand samples 1 and 2 possess different characteristics of grain size distribution as shown in Figure 4. In addition, Table 4 shows a summary of the fundamental material properties of sand samples 1 and 2. In the laboratory-scale chamber tests, the sand filter layers consist of one of the two sand samples or their combination.

LABORATORY CHAMBER TEST

Overview of laboratory-scale chamber tests

In order to evaluate the filtering performance of the sand filter layers that are assembled in the distributed rainwater reservoir, a laboratory-scale chamber with the dimensions of 20 cm × 30 cm × 60 cm was devised. An out-flow valve was installed at the lower part of the chamber to discharge the artificial urban runoff. The inside wall of the chamber was designed to be 5 cm lower than the outside wall to induce discharging of the overflow at the top of the inside wall. In an acrylic chamber, coarse grained aggregates were packed up to 40 cm thick. When the artificial runoff flowed into the chamber, it was distributed evenly into the filter layer to prevent piping through the filter layer. During the chamber test, the concentration of the artificial runoff was maintained as constant as possible by continually stirring the pollutant suspension inside the fiberglass reinforced plastic water tank with the capacity of 2 tons as shown in Figure 5. Considering the particle size of the non-point source pollutants suspended in the artificial runoff, a digital flow meter (E-MAG-I) was applied to measure flow rate.

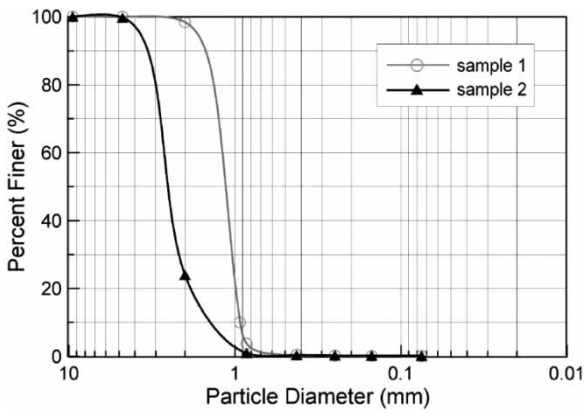

Figure 4 | Grain size distribution curves for filter layers (sample 1 and sample 2).

Three filter layers were considered in the laboratory-scale chamber test (refer to Table 5). Layer 1 consisted of sand sample 1 ($D_{10} = 0.93$ mm), and Layer 2 consisted of sand sample 2 ($D_{10} = 1.49$ mm). Layer 3 had two sub-layers: a lower layer of sand sample 1 and an upper layer of sand sample 2.

Table 4 | Material properties of sand filter layers (sample 1 and sample 2)

Soil property	Sample 1	Sample 2
Effective size (D_{10}, mm)	0.93	1.49
Uniformity coefficient (C_u)	1.65	2.01
Gradation coefficient (C_c)	0.96	1.08
Specific gravity (G_s)	2.74	2.63
Hydraulic conductivity (cm/s)	0.16	0.29

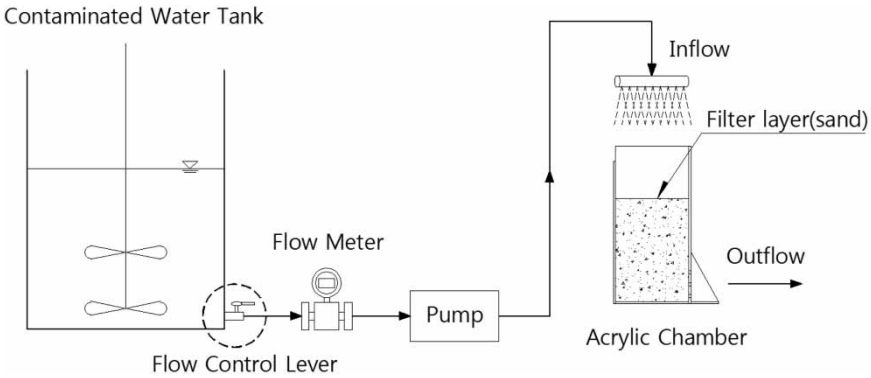

Figure 5 | Schematic diagram of laboratory-scale chamber system.

Table 5 | Three filter layers with different effective particle sizes and compositions

	Layer 1	Layer 2	Layer 3
Effective size (D_{10}, mm)	0.93	1.49	1.49 (upper layer), 0.93 (lower layer)

The artificial runoff was poured at a flow rate of 2 L/min for 10 minutes into the three types of sand filter layers. The pouring process was repeated more than 100 times for each filter layer. The TSS and COD of the inflow and outflow were monitored consecutively. In the case of Layer 1, the TSS and COD of the inflow and outflow artificial runoff were measured at 1, 5, 10, 20 and 30 cycles, and in the case of Layers 2 and 3, they were measured at 1, 5, 10, 20, 30, 40, 50, 60, 70, 80, 90 and 100 cycles. The TSS value was evaluated in accordance with the standard TSS analysis method for sediment concentration in water (ASTM 2007). The COD_{cr} value was measured with the aid of a COD LR kit from HACH to enhance test reproducibility.

Experimental results

The amount of the pollutant retained by the sand filter layers was evaluated by the difference in the TSS and COD (in particular COD_{cr} measured using the COD LR kit) values between the inflow and outflow artificial runoff. Figure 6 shows the change in pollutant concentration of TSS with an increase in pouring cycles during the chamber test, and Figure 7 shows that of COD.

In Layer 1, the measured TSS of the inflow artificial runoff ranged from 222 mg/L to 314 mg/L (average TSS was 275.7 mg/L), and the COD of the inflow artificial runoff was measured to be from 62.5 mg/L to 78 mg/L (average COD was 68.9 mg/L). The TSS of the outflow artificial runoff gradually decreased from 23.5 mg/L, and the COD of the outflow artificial runoff gradually decreased from 13 mg/L to 3 mg/L with increasing pouring cycles.

In Layer 2, the measured TSS of the inflow artificial runoff ranged from 159 mg/L to 294 mg/L (average TSS

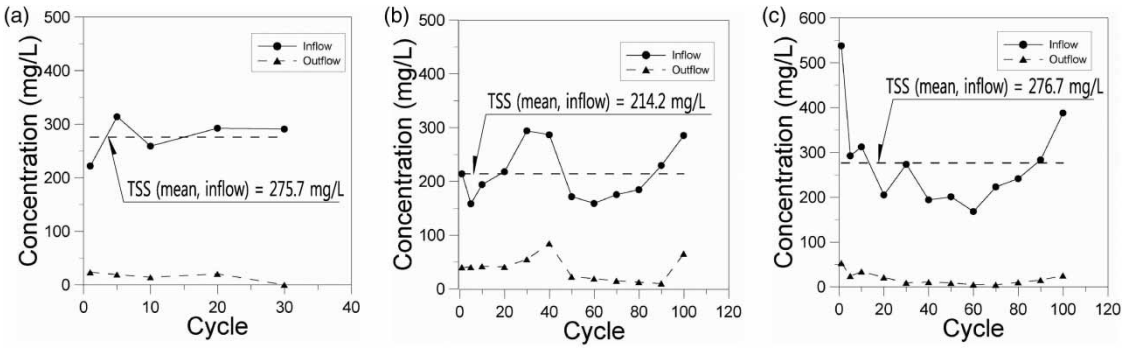

Figure 6 | Measurement of TSS with testing cycle: (a) Layer 1, (b) Layer 2, and (c) Layer 3.

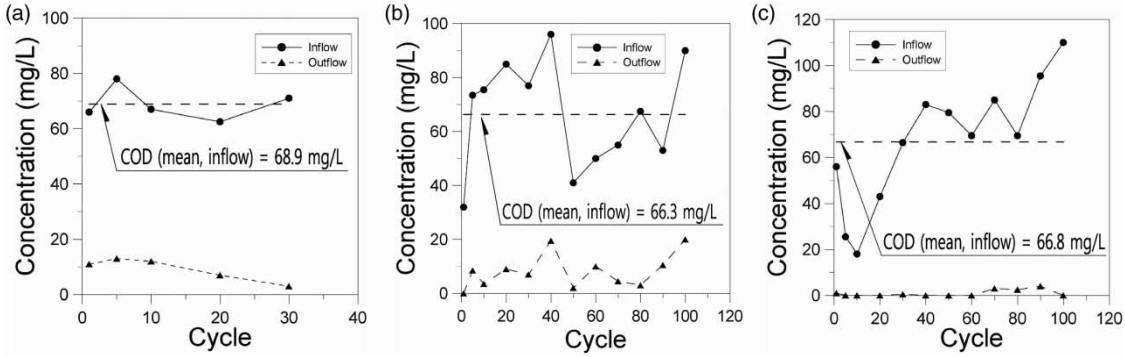

Figure 7 | Measurement of COD with testing cycle: (a) Layer 1, (b) Layer 2, and (c) Layer 3.

was 214.2 mg/L), and COD of the inflow artificial runoff was measured to be from 32 mg/L to 90 mg/L (average COD was 66.3 mg/L). With an increase in pouring cycles, the TSS of the outflow artificial runoff gradually decreased from 42 mg/L to 10 mg/L, and the COD of the outflow artificial runoff was measured to be less than 20 mg/L, but without an apparent tendency for a decrease in COD.

In Layer 3, the measured TSS of the inflow artificial runoff ranged from 168 mg/L to 538 mg/L (average TSS was 276.7 mg/L), and the COD of the inflow artificial runoff was measured from 18 mg/L to 110 mg/L (average COD was 66.8 mg/L). The TSS of the outflow artificial runoff gradually decreased from 53 mg/L to 4.5 mg/L up to the 70th cycle. However, there was a tendency for it to increase from 4.5 mg/L to 25 mg/L after the 70th cycle. Note that the TSS filtering capacity of Layer 3 is less than Layer 1 but greater than Layer 2. The COD of the outflow artificial runoff was measured to be less than 4 mg/L, indicating that most COD was removed through Layer 3 in consideration of the measurement precision of the COD LR kit of 3 mg/L to 150 mg/L.

The removal efficiency of the sand filter layers for non-point source pollutants can be estimated by normalizing the concentration difference in TSS or COD between the inflow and outflow artificial runoff as follows:

$$\text{Removal efficiency} = \frac{(C_{\text{in}} - C_{\text{out}})}{C_{\text{in}}} \tag{8}$$

where C_{in} is the concentration of the inflow, and C_{out} is the concentration of the outflow.

Figure 8 shows the removal efficiency of TSS with increasing pouring cycles during the chamber test, and Figure 9 shows that of COD.

In Layer 1, the TSS removal efficiency was shown to be more than 89%, and the COD removal efficiency ranged from 82% to 96%. The removal efficiency of both TSS and

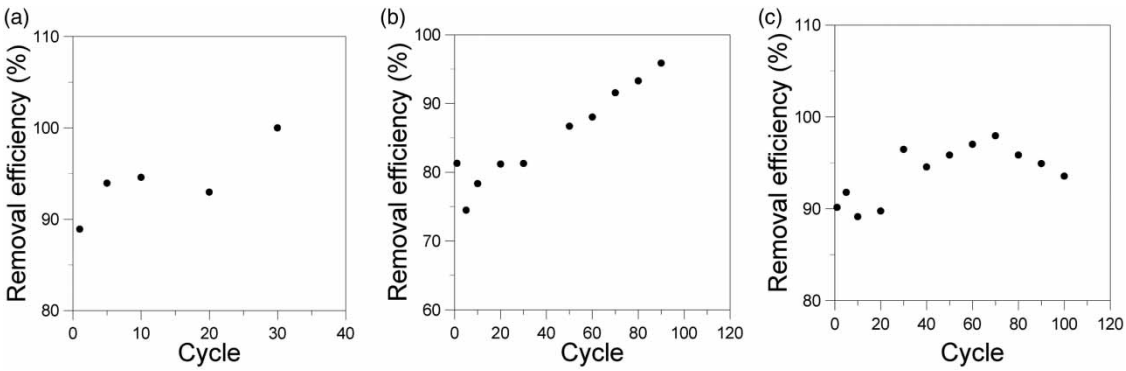

Figure 8 | Removal efficiency of TSS with testing cycle: (a) Layer 1, (b) Layer 2, and (c) Layer 3.

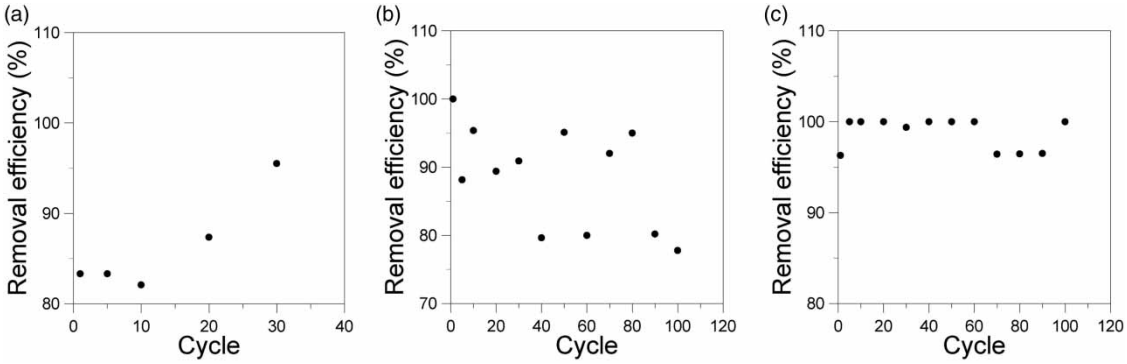

Figure 9 | Removal efficiency of COD with testing cycle; (a) Layer 1, (b) Layer 2, and (c) Layer 3.

COD increased with increasing pouring cycles. In Layer 2, the TSS removal efficiency showed a range from 74% to 96%, which increased as the pouring cycles increased. The COD removal efficiency was greater than 77% with slight scattering during the test, which seems to indicate that the COD removal capacity is not sufficient in Layer 2 which consists of relatively large size particles. In Layer 3, the TSS removal efficiency gradually increased from 89% to 98% before the 70th cycle. There was a slight fluctuation after the 70th cycle. It is thought that the TSS removal efficiency was slightly reduced corresponding to the measurement of the TSS. However, the TSS removal capacity of Layer 3 was fairly good because the TSS removal efficiency was maintained at more than 90% overall. The COD removal efficiency was more than 96%, which means outstanding filtering performance in all the testing cycles.

The total removed TSS can be calculated by accumulating the difference in TSS between the inflow and outflow artificial runoff, which is represented by Equation (9).

$$\text{Total removed TSS} = \sum [(\text{TSS of inflow} - \text{TSS of outflow}) \times \text{Inflow volume}] \quad (9)$$

The total removed TSS in the three sand filter layers is compared in Figure 10. Overall, the total removed TSS of each layer gradually increased with increasing pouring cycles. The total removed TSS was measured to be 159.6 g in Layer 1 (30 cycles), 358.1 g in Layer 2 (100 cycles) and 471.3 g in Layer 3 (100 cycles), which indicates that Layer 3 outperforms the other layers when removing TSS in the artificial runoff.

After completion of the laboratory-scale chamber tests, the non-point source pollutant particles clogged in the pores of the sand filter layer were carefully observed by producing an image of high resolution with the aid of a field emission scanning electron microscope (FE SEM) where

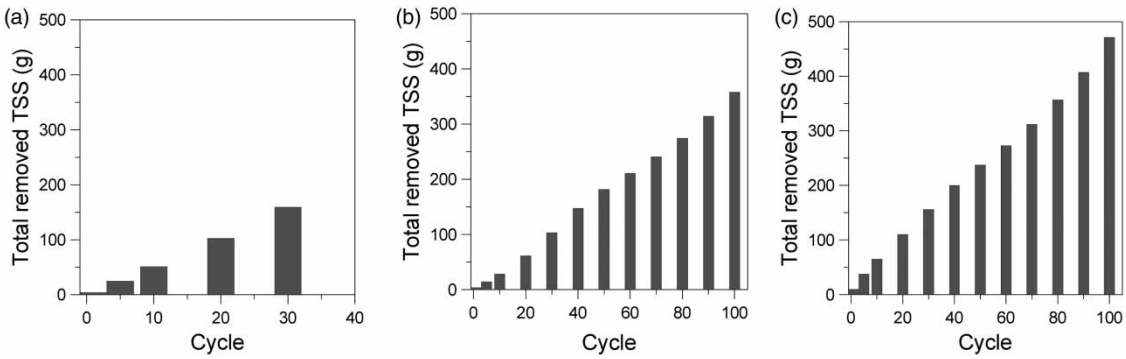

Figure 10 | Total removed TSS with testing cycle; (1) Layer 1, (b) Layer 2, and (c) Layer 3.

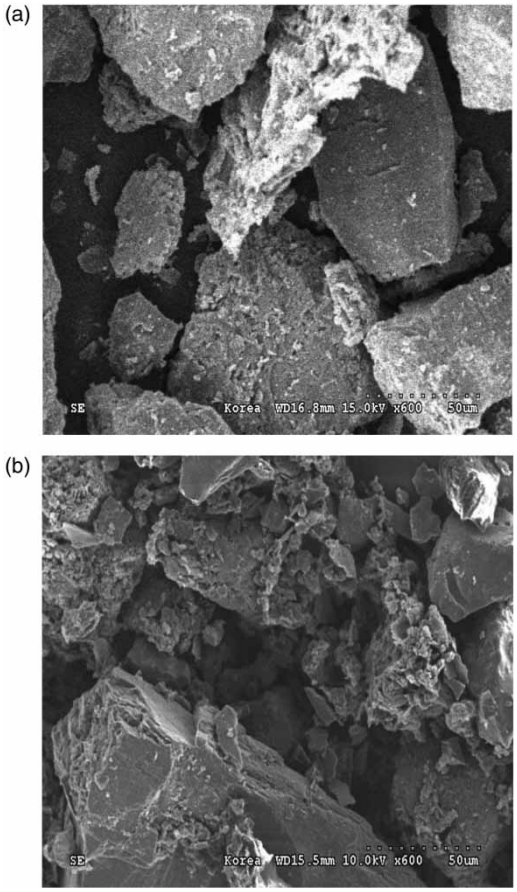

Figure 11 | Image of SEM (magnification of 600): (a) sand particles and (b) non-point source pollutant particles clogged in sand pores.

the magnification of images ranged from 50 to 1,500. Figure 11 shows the SEM images of the upper filter layer (effective grain size of 1.49 mm) in Layer 3 before the chamber test (Figure 11(a)) and after the chamber test (Figure 11(b)), which clearly exhibits fine pollutant particles clogged in the pores of the sand filter layer.

THEORETICAL VERIFICATION FOR LABORATORY-SCALE CHAMBER TEST RESULTS

In order to apply the analytical filtration model, the hydraulic characteristics of the filter medium should be determined at each pouring cycle. The hydraulic characteristics include the initial hydraulic conductivity and the variation of the porosity and hydraulic conductivity. The porosity of the filter medium is reduced with increasing pouring cycles due to the clogging phenomenon of the suspension, and the change in porosity can be expressed as follows (Kim *et al.* 2009):

$$n_{i+1} = n_0 - \frac{\bar{\sigma}_i}{G_s \cdot \gamma_w} \tag{10}$$

where n is the porosity (n_0 means the initial porosity), G_s is the specific gravity of pollutant particles, γ_w is the unit weight of water and the subscript i means the order of time step.

The change in intrinsic hydraulic conductivity (K_{int}) of the soil filter at the $(i+1)^{th}$ time step can be calculated using Equations (10) and (11) proposed by Kim *et al.* (2009). The variation of intrinsic hydraulic conductivity is formulated based on the Kozeny-Carman equation and expressed as Equation (11), considering the change of its void ratio and permeability, which is changed at the $(i+1)^{th}$ time step.

$$(K_{int})_{i+1} = (K_{int})_i \cdot \frac{(1-n_i)^2}{(n_i)^3} \cdot \frac{(n_{i+1})^3}{(1-n_{i+1})^2} \tag{11}$$

The updated values of porosity and intrinsic hydraulic conductivity obtained from Equations (10) and (11) are substituted into Equation (6) to obtain the amount of clogged suspension particles in the soil filter. The total accumulated deposition is then calculated by adding up the clogged particles in each cycle along with the fundamental material properties of the sand filter materials (i.e., the constants of m and b in Equation (7)).

Arya & Dierolf (1989) proposed Equation (12) to convert the radius of soil particles to the radius of pores.

$$r_i = \left[\frac{4 \cdot e \cdot R_i^3}{3 \cdot \alpha^*}\right]^{1/2} \tag{12}$$

where r_i is the radius of pores, R_i is the radius of soil particles, e is the void ratio, and α^* is the effective length of pore tubes. The value of α^* ranges from 3 mm for coarse sands to 15 mm for silts (Arya & Dierolf 1989). For the sand particles considered in this paper, an average value of α^* was determined to be 9.11 mm according to the inverse analysis of the grain size distribution. The grain size distribution of sands for the filter layer can be converted to the pore radius distribution using Equation (12). In addition, the standard deviation (b) of pore radii can be expressed

Table 6 | Influential factors adopted in clogging model for sand filter layers

Properties	Sample 1	Sample 2
Effective size (D_{10}, mm)	0.93	1.49
Hydraulic conductivity (cm/s)	0.157	0.294
m	−1.225	−0.414
b	0.309	0.624
Average size of migration particles	0.02	0.02
Specific gravity of pollutant particle	2.49	2.49
α^* (mm)	9.11	9.11
Initial concentration of contaminated water, C_0 (g/cm^3)	0.0003	0.0003

as Equation (13) along with the parameter of m that is an average value of ln(r) in a log normal distribution.

$$b = \sqrt{\sum (\ln r^2 \cdot s) - m^2} \tag{13}$$

where s is the frequency number. The parameters applied to the clogging model for each sand filter layer are summarized in Table 6.

The total removed TSS predicted from the clogging model is compared with the measurement from the laboratory-scale chamber test for varied lumped parameters (θ) in Figure 12. In this comparison, the well-fitted lumped parameter was estimated to be 3 for Layer 1 and 4.5 for Layer 2. On the other hand, for Layer 3, the lump parameter was 3 in the lower part and 4.5 in the upper part. In the clogging model, it is found that the lumped parameter θ increases with the effective grain size.

APPLICATION OF PILOT-SCALE FIELD SAND FILTER LAYER

Test bed construction

From the laboratory-scale chamber test, the double-sand-filter layer (Layer 3) was selected as the optimum sand filter layer and assembled in the pilot-scale distributed rainwater reservoir in a test bed. Applicability of the double-sand-filter layer was evaluated by performing a series of field tests. The test bed was built at a parking lot located in Gyeonggi-do, South Korea. The dimensions of the pilot-scale distributed rainwater reservoir are 4 m × 5 m for installing 21 storage cells, which covers rainfall on the designated parking area of 213 m^2.

The composition of the pilot-scale distributed rainwater reservoir installed in the test bed is illustrated in Figure 13. The reservoir system is composed of an infiltration well, which measures the removal ability of the sand filter layer, and 21 storage cells, which can store 20 tons of rainwater. The dimensions of the infiltration well are 1 m × 1 m × 2 m, and each storage cell is 1 m × 1 m × 1 m. In addition, the storage cells are made of concrete boxes that are connected to each other. The infiltration well consists of the double-sand-filter layer in the lower part along with a floating device to adjust the amount of inflow rainwater to cut off excessive inflow of rainwater over the designed water flow rate. The floating device was designed such that a rubber ball blocks the concave water way in the middle of the infiltration well corresponding to the rainwater level being raised up on the sand filter layer (refer to Figure 14).

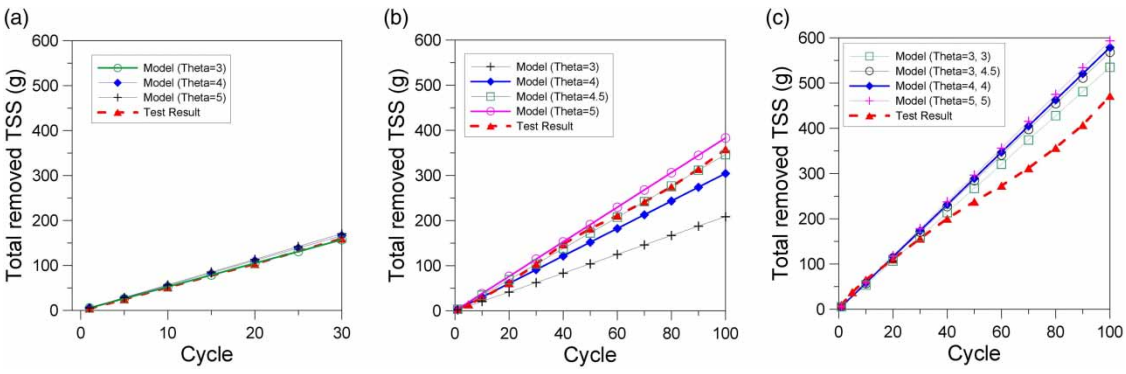

Figure 12 | Comparison of theoretical and measured values of total removed TSS for artificial urban runoff with non-point source pollutants; (a) Layer 1, (b) Layer 2, and (c) Layer 3.

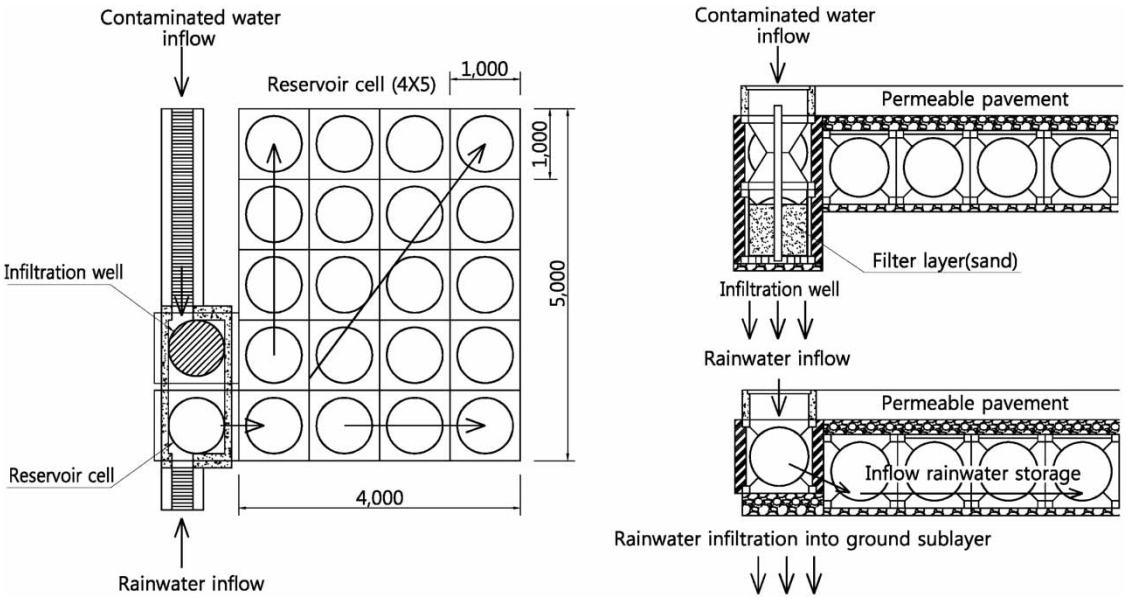

Figure 13 | Conceptual diagrams of pilot-scale rainwater reservoir.

The flow rate of the artificial urban runoff passing through the sand filter layer was determined to correspond to the rate of rainfall runoff induced by the initial rainfall of 5 mm in the target area. The rational method (Texas Department of Transportation 2014) was used to obtain the rainfall runoff around the test bed as follows:

$$\frac{1}{3.6}CIA \ (\mathrm{m}^3/\mathrm{s}) \tag{14}$$

where C is the runoff coefficient, I is the rainfall intensity (mm/h) and A is the target drain area (km^2). In this field test, C was selected to be 0.9 which corresponds to the maximum runoff for urban areas. I was designated as 5 mm/h, and the target drain area (A) was 213 m^2. The total amount of rainfall runoff for the first flush of 5 mm/h was calculated to be 0.960 m^3 (960 L).

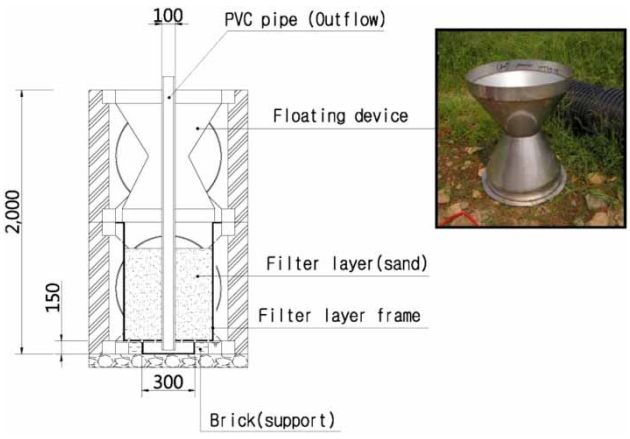

Figure 14 | Infiltration well with sand filter layer and floating device.

Field test program

The field test was performed in the following order: installing the sand filter layer into the infiltration well, setting the floating device and outflow pipe, mixing the non-point source pollutant sample with water, preparing the artificial urban runoff of the first flush, pouring the artificial urban runoff into the infiltration well, and monitoring the outflow as shown in Figure 15.

The artificial urban runoff with a TSS concentration of 100–400 mg/L was prepared by mixing the dry non-point source pollutants with water. In the mixing tank, a small stirrer was operated to prevent particles of the non-point source pollutants from forming sediment at the bottom. The artificial urban runoff was poured into the top of the pilot-scale rainwater reservoir. The outflow passing through the sand filter layer was then collected in a container. During the field test, the artificial urban runoff of 192 L was poured into the sand filter layer for each cycle, and this process

Figure 15 | Field test procedure to evaluate filtration efficiency of sand filter layer: (a) installing sand filter layer into infiltration well, (b) setting floating device and outflow pipe, (c) mixing non-point source pollutants sample with water, (d) preparing artificial urban runoff with non-point source pollutants, (e) pouring artificial urban runoff into infiltration well, and (f) monitoring outflow.

was repeated 50 times. The concentration of the inflow and outflow was evaluated in terms of the TSS and COD in each cycle.

Field test result

The removal efficiency of TSS and COD of the sand filter layer was evaluated by measuring the difference in the TSS and COD values between the inflow and outflow artificial runoff as shown in Figures 16 and 17. Figure 16 shows the change in pollutant concentration of TSS and COD with an increase in pouring cycles during the field test. The TSS of the inflow artificial runoff ranged from 114 mg/L to 365 mg/L (average TSS was 230.6 mg/L), and the COD of the inflow artificial runoff ranged from 54 mg/L to 140 mg/L (average COD was 105.1 mg/L). During the field test with an increase in pouring cycles, the TSS and turbidity of the outflow artificial runoff gradually decreased,

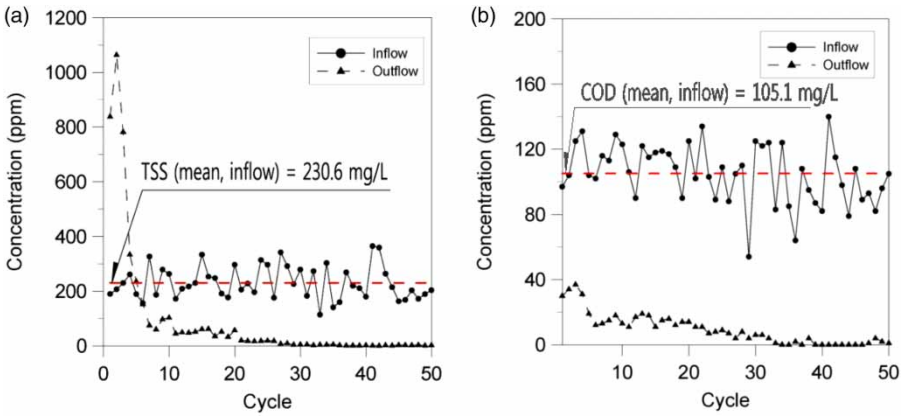

Figure 16 | Measurement of TSS and COD with testing cycles: (a) TSS and (b) COD.

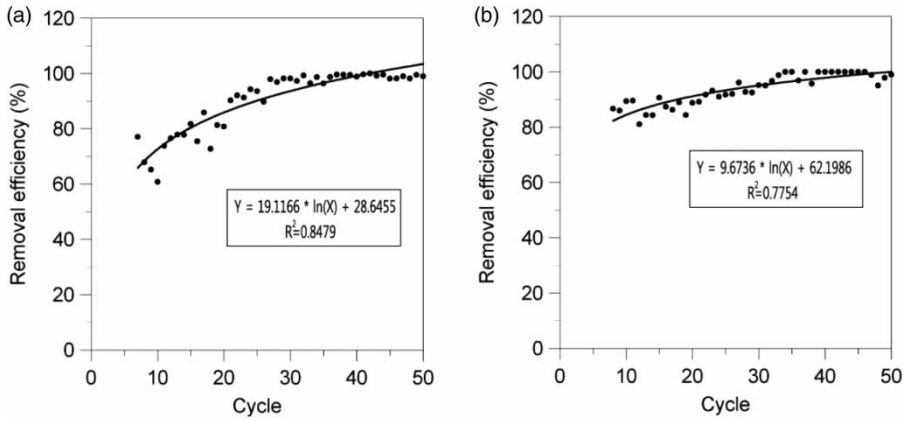

Figure 17 | Removal efficiency of TSS and COD with testing cycles: (a) TSS and (b) COD.

which means the non-point source pollutants were removed by the sand filter layer. In addition, the COD of the outflow artificial runoff also gradually decreased from about 37 mg/L at the beginning of the tests. Figure 17 shows the removal efficiency of TSS and COD according to the repeated inflow-outflow test. The TSS removal efficiency shows a range from 60.8% to 100% and the COD removal efficiency was more than 81.1% after 10 tests. The removal efficiency of TSS and COD increased with repeated test cycles.

The field test results for the double-sand-filter layer are compared with those of the laboratory-scale chamber test for Layer 3 and summarized in Table 7. The distributed rainwater reservoir consisting of the double-sand-filter layer constructed in the test bed satisfactorily performed the filtering function under natural rainfall conditions.

CONCLUSIONS

In this paper, the analytical filtration model for estimating the filtering capacity of a sand filter layer was verified by performing a series of laboratory-scale chamber tests and pilot-scale field tests. The laboratory-scale test considered three different sandfilter layers with different grain size characteristics and compositions. The performance of the sand filter layers was evaluated in terms of TSS and COD as the index of non-point source pollutants. The double-sand-filter layer (Layer 3) was selected as the optimum sand filter layer and assembled in the pilot-scale distributed

Table 7 | Comparison of TSS and COD measured from laboratory-scale chamber test and field test

TSS and COD value			Laboratory-scale chamber test	Field test
TSS	TSS^{a}_{inf} (mg/L)	Minimum	168.0	114.0
		Maximum	538.0	365.0
		Average	276.7	230.6
	TSS^{b}_{eff} (mg/L)	Minimum	4.5	1.0
		Maximum	53.0	152.0
		Cycle 10	34.0	103.0
		Cycle 30	9.0	5.0
		Cycle 50	8.5	2.0
		Cycle 80	10.0	–
	Removal of TSS (%)	Minimum	89.0	60.8
		Maximum	98.0	100.0
		Cycle 10	89.1	60.8
		Cycle 30	96.5	98.2
		Cycle 50	95.9	99.0
		Cycle 80	95.9	–
COD	COD^{a}_{inf} (mg/L)	Minimum	18.0	54.0
		Maximum	110.0	140.0
		Average	66.8	105.1
	COD^{b}_{eff} (mg/L)	Minimum	1.0	1.0
		Maximum	4.0	37.0
		Cycle 10	ND	13.0
		Cycle 30	ND	6.0
		Cycle 50	ND	1.0
		Cycle 80	2.5	–
	Removal of TSS (%)	Minimum	96.0	81.1
		Maximum	99.9	99.9
		Cycle 10	99.9	89.4
		Cycle 30	99.4	95.2
		Cycle 50	99.9	99.0
		Cycle 80	96.5	–
Total test cycle			100	50

ND, none detected.
[a]Influent.
[b]Effluent.

rainwater reservoir in a test bed. Applicability of the double-sand-filter layer was evaluated by performing a series of field tests. However, it is highly recommended to investigate the correlation between test cycles under the laboratory experiment condition and the life cycle of the sand filters in the rainwater reservoir under field conditions during rainfall. Some of the important findings are listed as follows:

1. Compared with Layer 1 and Layer 2, Layer 3 consisting of two sub-layers showed relatively excellent TSS removal capacity of more than 90% and COD removal capacity of more than 96%. Moreover, the total removed TSS was measured to be 159.6 g in Layer 1, 358.1 g in Layer 2 and 471.3 g in Layer 3. The results indicate that Layer 3 possesses outstanding filtering performance and it was therefore selected as the optimum sand filter layer and assembled in the pilot-scale distributed rainwater reservoir in a test bed.
2. The total removed TSS predicted from the theoretical clogging model was compared with the results of the laboratory-scale chamber test to back-analyze the lumped parameter (θ), which tended to increase with the effective grain size. The well-fitted lumped parameter was estimated to be 3 for Layer 1 and 4.5 for Layer 2. As for Layer 3, the lumped parameter was separately estimated to be 3 for the lower part and 4.5 for the upper part.
3. In the field test for the double-sand-filter layer, the TSS and COD of the outflow artificial runoff gradually decreased with an increase in pouring cycles. The TSS removal efficiency shows a range from 60.8% to 100%, and the COD removal efficiency was more than 81.1% after 10 tests. The removal efficiency of TSS and COD increased with repeated test cycles.

ACKNOWLEDGEMENTS

This work is supported by a Korea Agency for Infrastructure Technology Advancement (KAIA) grant funded by the Ministry of Land, Infrastructure and Transport (Grant 1615007273), and by the National Research Foundation of the Korean Government (NRF-2014R1A2A2A01007883).

REFERENCES

Anggraini, A. K., Fuchs, S. & Silva, A. 2014 Influence of effective size and level of supernatant layer in slow sand filter performance. *ASEAN Journal of Systems Engineering* **2** (2), 47–51.

Arya, L. M. & Dierolf, T. S. 1989 Predicting soil moisture characteristics from particle-size distributions: an improved method to calculate pore radii from particle radii. In: *Indirect Methods for Estimating the Hydraulic Properties of Unsaturated Soils (*M. T. Van Geuchten & F. J. Leij, eds). US Salinity Laboratory, Riverside, CA, pp. 115–124.

ASTM 2007 *Standard Test Methods for Determining Sediment Concentration in Water Samples, Designation: D 3977-97*. ASTM International, PA 19428-2959, USA.

Baek, S. S., Choi, D. H., Jung, J. W., Lee, H. J., Lee, H., Yoon, K. S. & Cho, K. H. 2015 Optimizing low impact development (LID) for stormwater runoff treatment in urban area, Korea: experimental and modeling approach. *Water Research* **86** (1), 122–131.

Bahgat, M., Dewedar, A. & Zayed, A. 1999 Sand filters used for wastewater treatment: build up and distribution of micro organisms. *Water Research* **33** (8), 1949–1955.

Barrett, M. E., Irish Jr, L. B., Malina Jr, J. F. & Charbeneau, R. J. 1998 Characterization of highway runoff in Austin, Texas, area. *Journal of Environmental Engineering* **124** (2), 131–137.

Caza, N., Bewtra, J. K., Biswas, N. & Taylor, K. E. 1999 Removal of phenolic compounds from synthetic wastewater using soybean peroxidase. *Water Research* **33** (13), 3012–3018.

Cho, K. W., Song, K. G., Cho, J. W., Kim, T. G. & Ahn, K. H. 2009 Removal of nitrogen by a layered soil infiltration system during intermittent storm events. *Chemosphere* **76**, 251–257.

Choi, J. Y. & Shin, E. S. 1997 *A study on management methods for non-point pollutants source in urban area*. Research Report, Korea Environment Institute, Sejong, Korea.

Gruesbeck, C. & Collins, R. E. 1982 Entrainment and deposition of fine particles in porous media. *Society of Petroleum Engineers Journal* **22** (6), 847–856.

Hori, T. S. F., Avilez, I. M., Inoue, L. K. & Moraes, G. 2006 Metabolical changes induced by chronic phenol exposure in matrinxa *Brycon cephalus* (teleostei: characidae) juveniles. *Comparative Biochemistry and Physiology, Part C: Toxicology & Pharmacology* **147** (4), 416–423.

Hsieh, C. & Davis, A. P. 2005 Evaluation and optimization of bioretention media for treatment of urban storm water runoff. *Journal of Environmental Engineering* **131** (11), 1521–1531.

Ives, K. J. 1987 Filtration of clay suspensions through sand. *Clay Minerals* **22**, 49–61.

John, J. S. & Steven, G. B. 1997 Partitioning and first flush of metals in urban roadway storm water. *Journal of Environmental Engineering* **123** (2), 134–143.

Kandra, H. S., Deletic, A. & McCarthy, D. 2014 Assessment of impact of filter design variables on clogging in stormwater filters. *Water Resources Management* **28** (7), 1873–1885.

Kim, J. S., Lee, I. M., Jang, J. H. & Choi, H. 2009 Groutability of cement-based grout with consideration of viscosity and filtration phenomenon. *International Journal for Numerical and Analytical Methods in Geomechanics* **33** (16), 1771–1797.

Kim, D. G., Kim, H. S., Kang, H. M. & Ko, S. O. 2016 Pollutant characteristics of road deposited sediments collected by road sweeping. *Water Science and Technology: Water Supply* **74** (1), 194–202.

Lee, I. M., Lee, S. & Cho, K. H. 2004 Face stability assessment of slurry-shield tunnels - concentrating on slurry clogging effect. *Journal of the Korean Geotechnical Society* **20** (6), 95–107 (In Korean).

Lee, D., Kim, K., Lee, H., Lim, J., Lee, I.-M. & Choi, H. 2016 Measurement of hydraulic properties of bentonite cake formation deposited on base soil medium. *Applied Clay Science* **123**, 187–201.

Liu, W., Chen, W., Peng, C., Wu, L. & Qian, Y. 2015 A water balance approach to assess rainwater availability potential in urban areas: the case of Beijing, China. *Water Science and Technology: Water Supply* **15** (3), 490–498.

Nair, A. T., Ahammed, M. M. & Davra, K. 2014 Influence of operating parameters on the performance of a household slow sand filter. *Water Science and Technology: Water Supply* **14** (4), 643–649.

Nguyen, T.-B., Lim, J., Choi, H. & Stark, T. D. 2011 Numerical modeling of diffusion for volatile organic compounds through composite landfill liner system. *KSCE Journal of Civil Engineering* **15** (6), 1033–1039.

Nieć, J., Spychała, M. & Zawadzki, P. 2016 New approach to modelling of sand filter clogging by septic tank effluent. *Journal of Ecological Engineering* **17** (2), 97–107.

Pitt, R. & Barron, P. 1990 *Assessment of Urban and Industrial Stormwater Runoff Toxicity and the Evaluation/ Development of Treatment for Runoff Toxicity Abatement-Phase I.* US EPA, Office of Research and Development, Edison, NJ, USA.

Reddi, L. N. & Bonala, M. V. S. 1997 Analytical solution for fine particle accumulation in soil filters. *Journal of Geotechnical and Geoenvironmental Engineering, ASCE* **123** (12), 1143–1152.

Rege, S. D. 1988 *Network Modeling and Experimental Investigation of Flow, Dissolution, Precipitation and Fines Migration in Porous Media*. PhD Dissertation, The University of Michigan, Ann Arbor, MI, USA.

Rege, S. D. & Fogler, H. S. 1988 A network model for deep bed filtration of solid particles and emulsion drops. *AIChe Journal* **34** (11), 1761–1772.

Rodgers, M., Mulqueen, J. & Healy, M. G. 2004 Surface clogging in an intermittent stratified sand filter. *Soil Science Society of America Journal* **68**, 1827–1832.

Schuetze, T. 2013 Rainwater harvesting and management-policy and regulations in Germany. *Water Science and Technology: Water Supply* **13** (2), 376–385.

Seigrist, R. L. & Boyle, W. C. 1987 Wastewater-induced soil clogging development. *Journal of Environmental Engineering* **113** (3), 550–566.

Stark, T. D., Choi, H. & Akhtarshard, R. 2004 Occurrence and effect of bentonite migration in geosynthetic clay liners. *Geosynthetics International, IFAI* **11** (4), 296–310.

Texas Department of Transportation 2014 *Hydraulic Design Manual*. Design Division, Austin, TX, USA.

Torben, L., Kirsten, B. & Margit, R. A. 1998 First flush effects in an urban catchment area in Aalborg. *Water Science and Technology* **37** (1), 251–257.

US EPA 1983 *Results of the Nationwide Urban Runoff Program*. Water Planning Division, PB 84-185552, Washington, DC, USA.

Wilson, C. E., Hunt lll, W. F., Winston, R. J. & Smith, P. 2014 Assessment of a rainwater harvesting system for pollutant mitigation at a commercial location in Raleigh, NC, USA. *Water Science and Technology: Water Supply* **14** (2), 283–290.

First received 7 February 2017; accepted in revised form 21 March 2017. Available online 9 May 2017